




Adsorptive Removal of Rhodamine B Dye from Aqueous Solutions Using Mineral Materials as Low-Cost Adsorbents

Krzysztof Kuśmierek · Joanna Fronczyk  · Andrzej Świątkowski

Received: 25 June 2022 / Accepted: 7 July 2023
© The Author(s) 2023

Abstract In this work, the potential adsorption abilities of mineral materials such as zeolite (Ze), halloysite (Ha), chalcedonite (Ch), and Devonian sand (DS) used as low-cost resources for the removal of Rhodamine B (RhB) from aqueous solutions were investigated in batch conditions. Adsorption kinetics and equilibrium and the effect of solution reaction (pH) were studied. Adsorption kinetic data were analyzed using two kinetic models: pseudo-first-order and pseudo-second-order models. Adsorption kinetics was better represented by the pseudo-second-order model. Equilibrium data were analyzed by the Freundlich, Langmuir, and Sips isotherms. The results show that equilibrium data fit well with the Freundlich equilibrium. Monolayer maximum adsorption capacities of RhB were assumed at 6.964, 4.252, 2.701, and 0.349 mg/g for Ze, Ha, Ch, and DS, respectively. Adsorption was strongly pH-dependent. The maximum RhB adsorption on all tested materials was observed at pH=2.2 and decreased with further pH increase. The results of these investigations

suggest that natural materials represented by certain minerals have a good potential for the removal of Rhodamine B from aqueous solutions.

Keywords Adsorption · Rhodamine B · Zeolite · Halloysite · Chalcedonite · Devonian sand

1 Introduction

For decades, the industrial, municipal, and agricultural activity of humans has resulted in the deterioration of various components of the natural environment. In addition to the introduction of harmful gases to the atmosphere, pollutants are also emitted to surface waters and subsoil, e.g., along with sewage or through illegal discharge, during industrial breakdowns and traffic accidents, industrial and municipal waste dumping, and use of chemicals in agriculture (Suthersan et al., 2016; Ukaogo et al., 2020; Wang et al., 2021). It is estimated that developing countries dominate in the emission of pollutants due to intensive industrial economies, while middle- and low-income countries contribute to this issue due to meeting immediate and basic human needs and the lack of funds for environmental purposes (Ukaogo et al., 2020). In addition, the lack of appropriate regulations and/or instruments to monitor compliance with environmental laws and the state of the environment is also of great importance (Ukaogo et al., 2020). The emission of pollutants, even to one environmental component, most often causes

K. Kuśmierek · A. Świątkowski
Faculty of Advanced Technologies and Chemistry,
Military University of Technology, 2 Kaliskiego Str.,
00-908 Warsaw, Poland

J. Fronczyk (✉)
Institute of Civil Engineering, Warsaw University
of Life Sciences – SGGW, 166 Nowoursynowska Str.,
02-787 Warsaw, Poland
e-mail: joanna_fronczyk@sggw.edu.pl

their spread to part or all of the remaining components. For example, pollutants from the soil may migrate to groundwater when clean water infiltrates through a contaminated zone or, in the presence of volatile substances, into the atmosphere during volatilization (Suthersan et al., 2016). In addition, pollutants passing through contaminated food to higher levels of the food chain are potentially dangerous to the health of animals and humans, resulting in, e.g., cancer, allergies, neurological changes, hormonal imbalance, reproductive impairment, or tissue damage (Long et al., 2021; Suthersan et al., 2016; Ukaogo et al., 2020).

The main types of pollutants ending up in the soil and water environment include inorganic pollutants (e.g., ammonia nitrogen and nitrogen oxides, phosphates, heavy metals) and organic pollutants (e.g., petroleum substances, hydrocarbons, pesticides, herbicides, pharmaceuticals) (Adebisi & Ayeni, 2021; Bandura et al., 2021; Bernasconi et al., 2021; Long et al., 2021). Remediation of contaminated sites, as well as surface and groundwater treatment, depends on the spectrum of pollutants present in the environment and the similarities or differences in their properties (Suthersan et al., 2016). Methods that can be used in practice are based on the susceptibility of chemicals to biological decomposition, sorption, or taking part in physicochemical reactions reducing the harmful effect of humans and other components of the environment. One of the solutions used in practice and analyzed on a laboratory scale is the use of synthetic and natural sorbents that effectively limit the spread of pollutants in the environment. While the synthesis or modification of materials often results in economic constraints and may be a potential source of emission of new pollutants, their large-scale use is often questioned. Hence, the use of low-cost mineral materials can be beneficial both from environmental and economic points of view (Radziemska et al., 2020a). Low-cost mineral materials can be used in many areas of environmental protection and engineering (Table 1). Radziemska et al., (2020a, b) demonstrated the potential applicability of diatomite, dolomite, halloysite, and chalcedonite to support the immobilization of heavy metals (Cd, Cr, Cu, Ni, Pb, Zn) in soil using an aided phytostabilization method. Additionally, these authors proved the application potential of diatomite, dolomite, and halloysite in the remediation of iron and steel scrap storage yards (Radziemska et al., 2019). Mineral materials were also used in the treatment of drinking water and

wastewater, e.g., Ukrainian tuff and basalt with zeolite were used to remove manganese (Trach et al., 2021); clinoptilolite was applied to remove lead ions (Reczek et al., 2014); dolomite — to remove phosphate (Piol et al., 2019); synthetic zeolite of NaP1 type to remove BTX (Bandura et al., 2017); zeolite to remove BTEX, PAHs, and MTBE (Vignola et al., 2011); and diatomite — in heavy metals removal (El Sayed, 2018). An interesting solution is the use of, e.g., zeolite (Birch et al., 2005; Fronczyk & Mumford, 2019; Fuerhacker et al., 2011), vermiculite (Fuerhacker et al., 2011), halloysite, diatomite, and limestone (Fronczyk & Mumford, 2019) for the treatment of runoff water from roads. Moreover, bentonites are widely used for environmental protection in the vicinity of landfills (Sieczka, 2015) and in removing various types of contaminants from aqueous solutions, including ciprofloxacin (Bizi & El Bachra, 2020), Cs-137, Am-241 ions (Oszczak-Nowińska et al., 2021), or Ph, BPA, 2,4-D, and IBU (Kuśmierek et al., 2020). It should be noted that the removal of Rhodamine B from aqueous solutions was also investigated. So far, the effectiveness of removing this organic compound has been confirmed for diatomite (Koyuncu & Kul, 2014), perlite (Vijayakumar et al., 2012), various natural and modified bentonites (de Moraes Pinos et al., 2022; Hakim et al., 2023; Lamrani et al., 2023; Zimmermann et al., 2016), barite (Vijayakumar et al., 2010), kaolin (He et al., 2022), and modified halloysites (Wierzbicka et al., 2022). Taking into account the potential of raw materials, it seems justified to conduct further research on their ability to remove organic impurities from aqueous solutions.

The present investigation was focused on the adsorption potential of low-cost, locally available, natural materials such as zeolite (Ze), halloysite (Ha), chalcedonite (Ch), and Devonian sand (DS) in the uptake of Rhodamine B (RhB), which was selected as the model pollutant. Rhodamine B is an important cationic dye that is widely used in the paper, paint, and textile industries (Vieira et al., 2020) and as a biological stain in laboratories (Liu et al., 2015). Moreover, due to its high-water solubility and strong fluorescence even at low concentrations, RhB is commonly used as a tracer dye in various aquatic media to determine the rate and direction of flow and transport (Skjolding et al., 2021). Rhodamine B, like most synthetic dyes, is highly toxic to various organisms and is suspected of having carcinogenic effects (Liu et al., 2015; Skjolding et al.,

Table 1 List of selected natural minerals together with the branch of their application and the pollutants removed

Mineral material	Field of application	Pollutant	Source
Diatomite Dolomite Halloysite	Aided phytostabilization	Cd, Cr, Cu, Ni, Pb, Zn	Radziemska et al. (2020a)
Chalcedonite Halloysite	Soil remediation	Cd, Cr, Cu, Ni, Pb, Zn	Radziemska et al. (2020b)
Diatomite Dolomite Halloysite	Iron and steel scrap storage yard remediation	Cd, Cr, Cu, Ni, Pb, Zn	Radziemska et al. (2019)
Ukrainian tuff Basalt	Water treatment	Manganese	Trach et al. (2021)
Clinoptilolite	Water treatment	Pb ²⁺	Reczek et al. (2014)
Dolomite	Water treatment	Phosphate	Piol et al. (2019)
Diatomite	Water and wastewater treatment	Ba, Cd, Al., Cr, Cu, Fe, Pb, Mn, Ni, Zn	El Sayed, 2018
Zeolite Quartz	Stormwater treatment	NO ₃ ⁻ , TKN, TP, fecal coliforms, trace metals (Cd, Cr, Cu, Fe, Mn, Ni, Pb, Zn), organochlorines, PCBs, PAHs, methylnaphthalene, oil, grease	Birch et al. (2005)
Vermiculite Zeolite	Stormwater treatment	PAHs, mineral oil, TOC, TSS, NH ₄ , chlorides, total and dissolved heavy metals (Cd, Cu, Zn)	Fuerhacker et al. (2011)
Diatomite Zeolite Halloysite Limestone	Stormwater treatment	Cd, Cu, Ni, Pb, Zn	Fronczyk and Mumford (2019)
Diatomite Kaolin Bentonites rich in montmorillonite	Aqueous solution treatment	Ciprofloxacin	Bizi and El Bachra (2020)
Bentonites	Aqueous solution treatment	Radionuclides Cs-137, Am-241 ions	Oszczak-Nowińska et al. (2021)
Bentonites	Low-cost adsorbents	Ph, BPA, 2,4-D, IBU	Kuśmierk et al. (2020)
Diatomite	Aqueous solution treatment	Rhodamine B	Koyuncu and Kul (2014)
Perlite	Aqueous solution treatment	Rhodamine B	Vijayakumar et al. (2012)
Brazilian natural bentonite	Aqueous solution treatment	Rhodamine B	Zimmermann et al. (2016)
Barite	Aqueous solution treatment	Rhodamine B	Vijayakumar et al. (2010)

2021). Therefore, its removal from industry effluents and aquatic environments is very important due to its highly negative impact.

2 Materials and Methods

2.1 Materials

The Rhodamine B dye (RhB, CAS number: 81–88-9) was purchased from Sigma-Aldrich (St Louis, MO, USA). All

other chemicals used in this work were purchased from Avantor Performance Materials (Gliwice, Poland).

Samples of mineral materials were obtained from local deposits. Zeolite (Ze) came from the Niżny Hrabovec deposit (Bystre, Slovakia), Devonian sand (DS) was obtained from the deposits located in south-eastern Poland, chalcedonite (Ch) was from Chalcedon Poland (Inowłódz, Poland), while halloysite (Ha) was obtained from the “Dunino” mine (Legnica, Poland). The raw materials were dried in an oven at 120 °C to a constant weight and stored in

a desiccator until use. Detailed characteristics of the zeolite and halloysite properties were presented by Fronczyk (2020).

2.2 Adsorbents Characteristics

The nitrogen adsorption–desorption isotherm of the tested materials was determined at 77 K using ASAP 2020 by Micromeritics (Norcross, GA, USA). The results obtained were the basis for the specific surface area (S_{BET}) calculations using the Brunauer–Emmett–Teller (BET) method. Volumes of micropores (V_{mi}) and mesopores (V_{me}) were also calculated.

Surface morphology and elemental composition of the applied materials were analyzed using scanning electron microscopy with energy dispersive spectroscopy (FEG Quanta 250, USA).

The mineral composition of the tested materials was determined using a Panalytical X'pertPRO MPD X-ray diffractometer (Panalytical) with a PW 3020 goniometer (Panalytical) and a Cu copper lamp ($CuK\alpha = 1.54178 \text{ \AA}$) as the source of X-ray emission. X'Pert Highscore software was used to process diffraction data, and the PDF-2 Release 2010 database (formalized by JCPDS-ICDD) was applied to identify the mineral phases.

The point of zero charge (pH_{pzc}) of the materials was also determined. The pH of 20 mL of 0.01 mol/L NaCl solution within each Erlenmeyer flask was adjusted to values ranging from 2 to 12 by 0.1 mol/L NaOH and/or 0.1 mol/L HCl. Then, 0.05 g of the materials was added. All the flasks were shaken for 24 h, and the pH of the solution was measured. The graph of final pH vs. initial pH was used to determine the point at which the initial pH and final pH of the adsorbent solution were equal.

2.3 Batch Adsorption Studies

Adsorption studies of RhB from aqueous solutions onto halloysite, zeolite, chalcedonite, and Devonian sand were performed at 25 °C using the batch equilibrium method. The experiments were carried out by mixing adsorbents (0.02 g of Ze or Ha and 0.05 g of DS or Ch) with RhB solution (10 mL) of an appropriate concentration in Erlenmeyer flasks

and agitated at 100 rpm. Finally, the adsorbents were separated from the solution, and the RhB concentration was analyzed using a UV–visible spectrophotometer (Carry 3E, Varian, USA) at 554 nm wavelength. The calibration curve used to measure the RhB concentration was linear in the tested range (from 0.05 to 20 $\mu\text{mol/L}$), with a correlation coefficient R^2 at 0.998. The equation for the regression line was $y = 0.079x + 0.025$.

The kinetic experiments were conducted for an initial dye concentration of 15 $\mu\text{mol/L}$. Samples at different time intervals were withdrawn and filtrated, and the dye solution was analyzed for residual RhB concentration. Equilibrium isotherms were determined by varying the initial dye concentration in the range of 2–20 $\mu\text{mol/L}$. The natural pH of the dye solution ($\text{pH} = 4.6$) was selected for the subsequent kinetic and equilibrium studies. To study the effect of pH, a series of solutions (10 mL) of 10 $\mu\text{mol/L}$ of RhB was adjusted to different pH values (2.2–9.5) using 0.1 mol/L HCl or 0.1 mol/L NaOH. After the addition of the adsorbates, samples were agitated for 24 h.

The amount of RhB adsorbed at time t , q_t ($\mu\text{mol/g}$), and at equilibrium q_e ($\mu\text{mol/g}$), as well as the percentage of dye removal, was calculated using the following equations:

$$q_t = \frac{(C_0 - C_t)V}{m} \quad (1)$$

$$q_e = \frac{(C_0 - C_e)V}{m} \quad (2)$$

$$\% \text{ Removal} = \frac{(C_0 - C_e)}{C_0} \times 100 \quad (3)$$

where C_0 , C_t and C_e represent the initial adsorbate concentration, the concentration at time t , and the equilibrium concentration of adsorbate in the solution ($\mu\text{mol/L}$), respectively; V is the solution volume (L), and m is the adsorbent mass (g).

To investigate the kinetic behavior of RhB adsorption, experimental data was applied to the pseudo-first-order (Eq. (4)) and pseudo-second-order (Eq. (5)) kinetic models (Tan & Hameed, 2017):

$$\log(q_e - q_t) = \log q_e - \frac{k_1}{2.303} t \quad (4)$$

$$\frac{t}{q_t} = \frac{1}{k_2 q_e^2} + \frac{1}{q_e} t \quad (5)$$

where k_1 is the pseudo-first-order rate constant (1/min) and k_2 is the pseudo-second-order rate constant ($\text{g}/\mu\text{mol}\cdot\text{min}$).

The equilibrium data were tested using three isotherm models, i.e., Freundlich, Langmuir, and Sips (Ayawei et al., 2017; Al-Ghouti & Da'ana, 2020).

The Freundlich model is presented in Eq. (6):

$$q_e = K_F C_e^{1/n} \quad (6)$$

where K_F ($(\mu\text{mol}/\text{g})(\text{L}/\mu\text{mol})^{1/n}$) and n are the Freundlich constants.

The Langmuir model is presented in Eq. (7):

$$q_e = \frac{q_{mL} K_L C_e}{1 + K_L C_e} \quad (7)$$

where q_{mL} is the maximum adsorption capacity ($\mu\text{mol}/\text{g}$), and K_L is the Langmuir constant ($\text{L}/\mu\text{mol}$).

Equation (8) presents the Sips isotherm:

$$q_e = \frac{q_{mS} K_S C_e^m}{1 + K_S C_e^m} \quad (8)$$

where q_{mS} is the Sips maximum adsorption capacity ($\mu\text{mol}/\text{g}$), K_S is the Sips equilibrium constant ($\text{L}/\mu\text{mol}$) ^{m} , and m is the Sips model constant.

The correlation coefficients (R^2), along with the chi-square tests (χ^2), were applied to determine the model that best fitted the experimental data. A lower value of χ^2 and a higher value of R^2 indicate a good fit between the experimental and calculated data.

All the experiments were carried out in duplicate replications, and the reported values correspond to the average.

3 Results and Discussion

3.1 Physicochemical Characteristics of the Adsorbents

Nitrogen adsorption–desorption isotherms and textural properties of mineral materials tested are presented in Fig. 1 and Table 2, respectively. Zeolite, halloysite, and chalcedonite represent mesoporous materials with a moderately developed specific

surface and mesopores being narrow slits of irregular size and shape. In turn, Devonian sand can be considered a non-porous material. The highest specific surface area and total volume of pores were determined for the halloysite, followed by zeolite. Much lower values of these parameters were measured for chalcedonite and Devonian sand.

SEM images (Fig. 2) confirmed the moderately extensive surfaces of zeolite and halloysite, and in the case of the latter material, the presence of characteristic nanotubes, which, however, are usually not clearly visible at such magnification. The microscopic image of chalcedonite shows irregularly distributed, strongly jagged thin plaques of clay minerals — mainly kaolinite. In the SEM image of Devonian sand, small amounts of lamellar clay minerals (illite) occur apart from calcite, which is in the form of irregular clusters. The composition of the sample surfaces from EDS is listed in Table 3.

The results of the XRD tests are presented in Fig. 3. The test results for halloysite confirm the presence of this mineral and the admixtures — goethite, hematite, and microclines. The main component of zeolite is clinoptilolite. Additionally, quartz and illite were observed in the sample. The mineral composition of chalcedonite is dominated by quartz, accompanied by the clay mineral kaolinite. The performed preparation required in the clay mineral tests, related to sample ignition at the temperature of 550 °C, confirmed the presence of this mineral. This is due to the

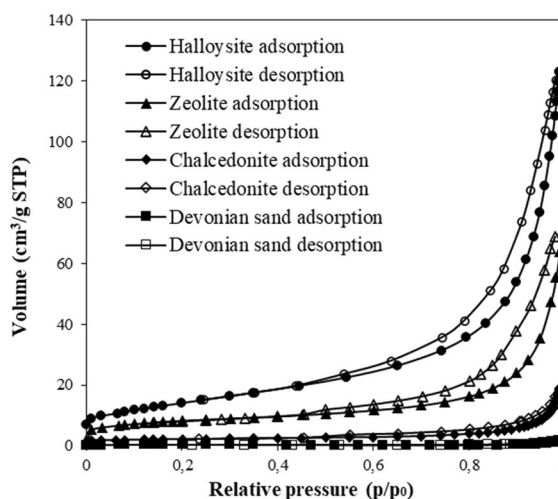


Fig. 1 Nitrogen adsorption–desorption isotherms (measured at 77 K) of the tested mineral materials

Table 2 Textural properties of halloysite, zeolite, chalcedonite, and Devonian sand

Sorbent	S_{BET} (m^2/g)	V_t (cm^3/g)	V_{mi} (cm^3/g)	V_{me} (cm^3/g)
Zeolite	33.3 ¹	0.110	0.0128 (11.6%)	0.0972 (88.4%)
Halloysite	51.4 ²	0.189	0.0225 (11.8%)	0.167 (88.2%)
Chalcedonite	7.44 ³	0.0291	0.0038 (13.1%)	0.0253 (86.9%)
Devonian sand	1.22 ⁴	0.0029	0.00052 (17.9%)	0.00238 (82.1%)

¹Fronczyk and Garbulewski (2013)

²Fronczyk and Mumford (2019)

³Fronczyk et al. (2014)

⁴Fronczyk and Radziemska (2016)

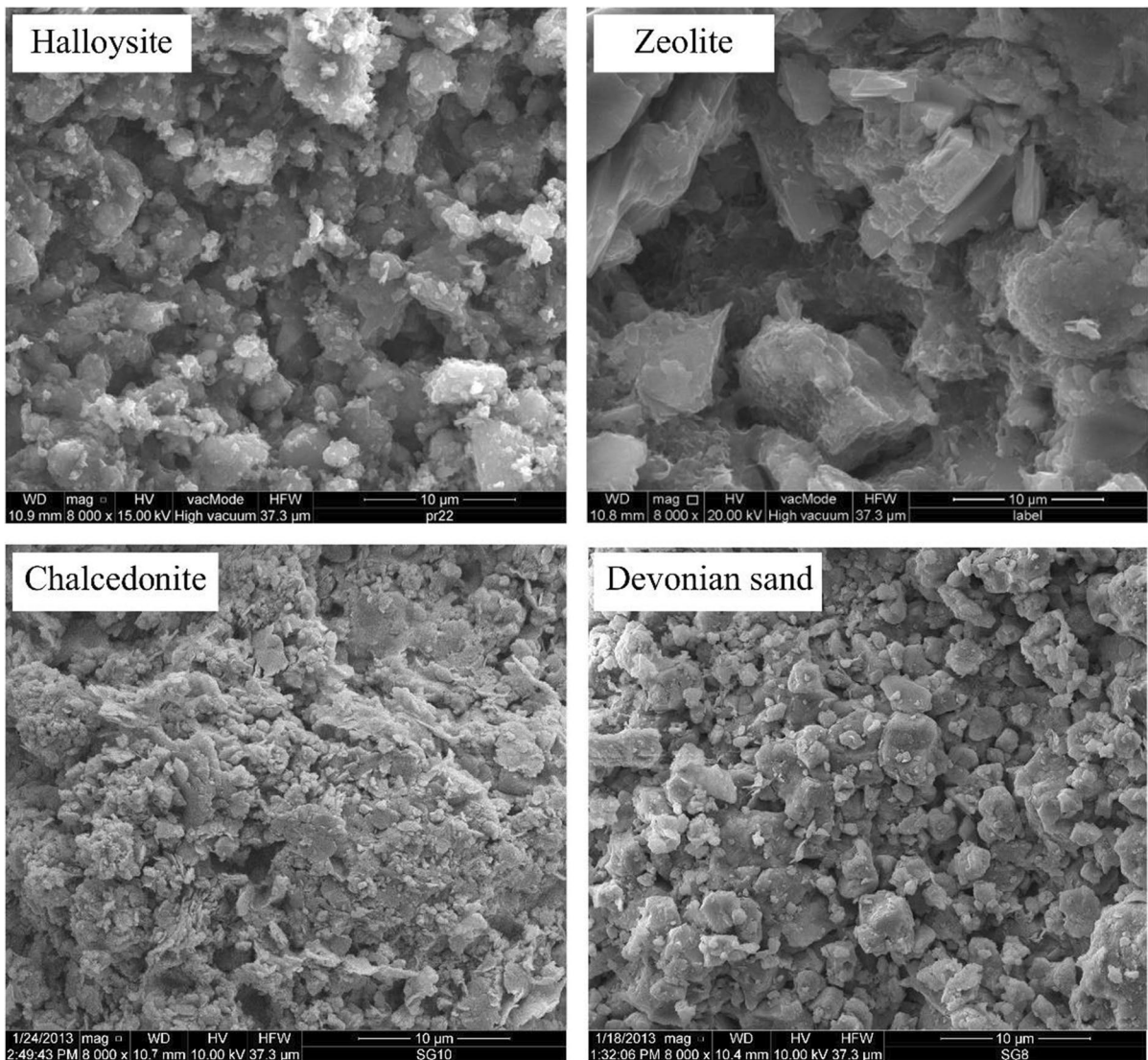
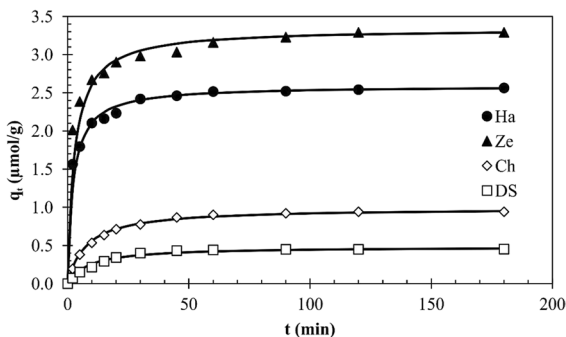
**Fig. 2** SEM images of the tested mineral materials (magnification x8000)

Table 3 Results of EDS analysis of the tested mineral materials samples

Sorbent	Chemical composition (wt%)											
	O	Ca	Si	Al	Mg	Fe	K	Cu	Pb	Ti	P	N
Zeolite	47.62		33.18	8.79	0.356	0.357	0.996	0.655	8.05			
Halloysite	47.30	0.865	19.36	22.17	0.199	7.826				2.02	0.262	
Chalcedonite	49.85		36.40	5.282	0.241	8.212						
Devonian sand	44.46	34.13	4.047	2.99	0.975	3.864		2.282				7.247

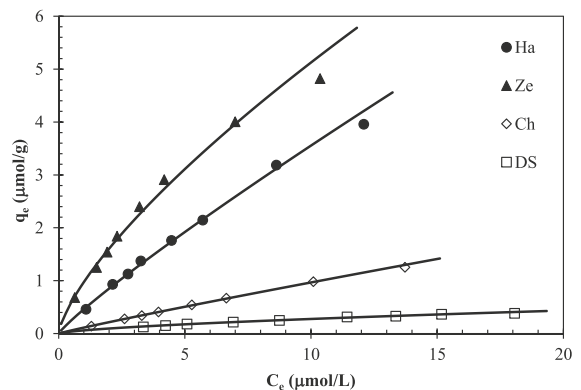
**Fig. 3** Adsorption kinetics of Rhodamine B on the tested mineral materials (line — fitting of pseudo-second-order kinetic model)

lack of reflections after the ignition process, which makes it possible to distinguish it from chlorite. The main mineral in Devonian sand is calcite. It is accompanied by small amounts of dolomite.

3.2 Adsorption Kinetics

The adsorption kinetic curves of RhB onto halloysite, zeolite, chalcedonite, and Devonian sand were obtained at an initial dye concentration of 15 $\mu\text{mol/L}$ and are presented in Fig. 3. RhB adsorption on the materials was a rapid process; more than 90% of dye was removed after about 15 min. Afterward, the adsorption rate decreased considerably, with the equilibrium reached after 90–120 min.

Kinetic parameters for both pseudo-first-order and pseudo-second-order models are listed in Table 4. The correlation coefficient values for pseudo-second-order kinetics (≥ 0.998) were higher than for pseudo-first-order kinetics. The chi-square values for the pseudo-second-order were found to be much lower (≤ 0.032) than those obtained for the pseudo-first-order equation. Moreover, equilibrium

**Fig. 4** Adsorption isotherms of Rhodamine B from aqueous solution on the mineral materials (line — fitting of Freundlich isotherm)

adsorption capacities (q_{e2}) for pseudo-second-order kinetics are more reasonable than those for pseudo-first-order kinetics (q_{e1}) when the predicted results are compared with experimental data ($q_{e\text{exp}}$). This suggests that pseudo-second-order kinetics was more appropriate to represent data from the adsorption of RhB on all the materials. The Devonian sand displayed the fastest rate of dye removal (k_2), followed by halloysite > chalcedonite > zeolite.

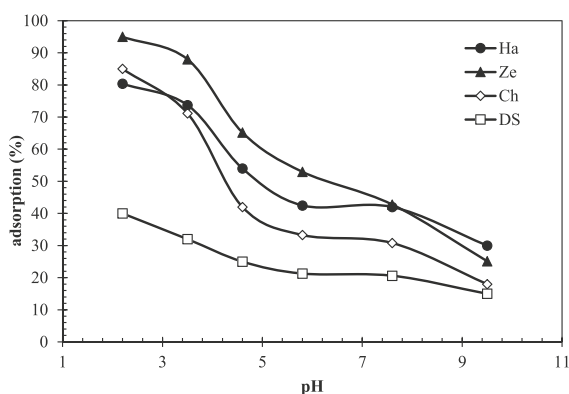
3.3 Adsorption Isotherms

Figure 4 shows the equilibrium RhB adsorption on the four mineral materials. The Freundlich, Langmuir, and Sips model parameters were evaluated by non-linear regression using OriginPro 8.0 software; the results are listed in Table 5.

The most efficient RhB removal was observed using zeolite, while the dye was most weakly adsorbed on Devonian sand. The calculated K_F , q_{mL} , and q_{mS} constants increased in the following order:

Table 4 Kinetic model parameters for Rhodamine B adsorption on the tested mineral materials

Kinetic model	Adsorbent			
	Halloysite	Zeolite	Chalcedonite	Devonian sand
Pseudo-first model				
k_1 (1/min)	0.036	0.036	0.044	0.051
q_{e1} ($\mu\text{mol/g}$)	0.803	1.218	0.674	0.327
R^2	0.916	0.905	0.955	0.967
χ^2	12.40	11.86	8.051	7.089
Pseudo-second model				
k_2 ($\text{g}/\mu\text{mol}\cdot\text{min}$)	0.165	0.105	0.131	0.191
q_{e2} ($\mu\text{mol/g}$)	2.593	3.340	0.991	0.481
R^2	0.999	0.998	0.999	0.999
χ^2	0.012	0.032	0.018	0.009
$q_{e\text{exp}}$ ($\mu\text{mol/g}$)	2.562	3.291	0.942	0.451

**Fig. 5** Effect of solution pH on adsorption of Rhodamine B on the mineral materials

$DS < Ch < Ha < Ze$. The relatively poor adsorption of RhB on DS and Ch is probably due to the low porosity of these materials. However, porosity does not fully explain dye adsorption on Ze and Ha. If only the BET surface area of the adsorbents is taken into account, the dye should be adsorbed better on halloysite, which has a larger specific surface area ($51.4 \text{ m}^2/\text{g}$) than zeolite ($33.3 \text{ m}^2/\text{g}$). Meanwhile, a reverse order can be observed — RhB was adsorbed better by zeolite despite its lower porosity compared to the halloysite. This suggests that adsorption not only is dependent on the textural properties of the adsorbents, but that surface charge and chemistry also play an important role. Unfortunately, the mechanisms of RhB adsorption on the tested materials have never been clearly described and require further research.

The results presented in Table 5 also show that all three models fairly well described the adsorption process. However, the Freundlich model exhibited slightly better correlation coefficients (≥ 0.993) and lower chi-square values (≤ 0.009) than the other models. Both the Langmuir and Sips isotherms produced slightly lower R^2 and higher χ^2 values. The Freundlich isotherm considers multilayer adsorption in multiple layers with a heterogeneous energy distribution of the active sites, as well as interactions between the adsorbed molecules. The Langmuir theoretical isotherm assumes a surface with homogeneous binding sites that suggest that adsorption takes place onto a uniform site. The Sips equation is a combination of the Freundlich and Langmuir isotherms and assumes that the mechanism of adsorption is a hybrid and does not follow ideal monolayer adsorption (Al-Ghouti & Da'ana, 2020; Aya-wei et al., 2017). The good fit obtained with the Freundlich model suggests that the adsorption of Rhodamine B onto Ha, Ze, Ch, and DS was physical. Moreover, adsorption may involve multi-layer adsorption with interactions between the RhB molecules, and the heterogeneous nature of the mineral surfaces is also implied.

Table 6 summarizes a comparison of the adsorption capacity of the tested mineral materials with others found in the literature. As can be seen, the adsorption capacity for the most efficient of the tested materials (zeolite) is 6.964 mg/g and is better than the adsorption capacity of sugar cane bagasse (Abou-Gamra & Medien, 2013), raw walnut shells

Table 5 Isotherm parameters of Rhodamine B adsorption on the tested mineral materials

Isotherm model	Adsorbent			
	Halloysite	Zeolite	Chalcedonite	Devonian sand
Freundlich				
$K_F ((\mu\text{mol/g})(\text{L}/\mu\text{mol})^{1/n})$	0.458	0.974	0.113	0.061
n	1.124	1.387	1.073	1.519
R^2	0.996	0.993	0.997	0.993
χ^2	0.004	0.008	0.003	0.009
Langmuir				
$q_{mL} (\mu\text{mol/g})$	8.877	14.54	5.639	0.728
$K_L (\text{L}/\mu\text{mol})$	0.031	0.117	0.014	0.064
R^2	0.942	0.979	0.975	0.971
χ^2	0.034	0.023	0.025	0.019
Sips				
$q_{mS} (\mu\text{mol/g})$	8.660	12.59	5.375	1.270
$K_S (\text{L}/\mu\text{mol})^m$	0.035	0.122	0.023	0.022
m	1.034	1.025	1.044	0.828
R^2	0.988	0.987	0.990	0.986
χ^2	0.013	0.012	0.012	0.014

(Shah et al., 2013), fly ash (Khan et al., 2009), ultrasound, and sulfuric acid-treated halloysites (Wierzbicka et al., 2022) and is comparable to natural pomegranate peels ground powder (Saigl & Ahmed, 2021), modified zeolite (mordenite) (Cheng et al., 2016), diatomite (Koyuncu & Kul, 2014), and kaolin (He et al., 2022). Other sorbents presented in Table 6 showed a better ability for RhB uptake from water. Other sorbents presented in Table 6 showed a better ability for RhB uptake from water. Despite this, the adsorption capacity of the tested materials, especially zeolite and halloysite, is satisfactory, which makes them effective and promising sorbents useful in removing dye from water. The use of these materials as sorbents for RhB removal is commercially viable because of their low cost and large availability.

3.4 Effect of pH on Rhodamine B Adsorption

The effects of solution pH on the adsorption of RhB on zeolite, halloysite, chalcedonite, and Devonian sand were investigated within the pH range of 2.2–9.5; the results are presented in Fig. 5. The maximum percentage of dye removal was obtained at pH 2.2, after which the percentage adsorption decreased significantly. When the pH increased from 2.2 to 9.5, RhB adsorption decreased from

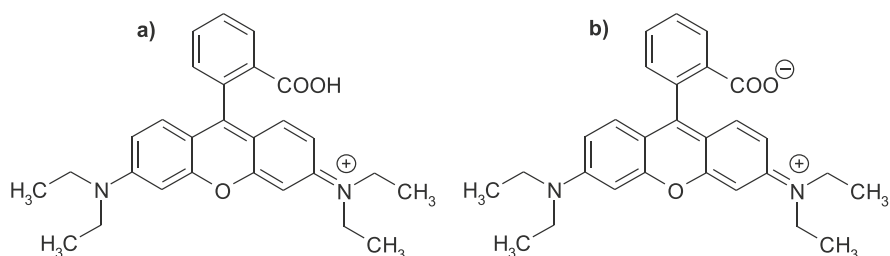
95.0 to 21.5% for Ze, from 40.0 to 15.1% for DS, from 85.0 to 18.2% for Ch, and from 84.0 to 30.1% for Ha, respectively.

The results show that the percentage of dye removal strongly depends on the pH of the solution. The pH determines the charge on the adsorbent surface, as well as the form in which the dye exists in the solution. The point of zero charge (pH_{pzc}) is defined as the pH value at which the liquid phase charge of the adsorbent is equal to zero. At a $\text{pH} < \text{pH}_{\text{pzc}}$, the adsorbent surface is positively charged, while at $\text{pH} > \text{pH}_{\text{pzc}}$, the surface has a net negative charge. The pH_{pzc} values of Ze, Ha, Ch, and DS were noted at 6.3, 6.5, 7.7, and 7.9, respectively. RhB is a cationic dye that may exhibit different molecular forms in different pH solutions. The carboxyl group of its structure has pK_a 3.7, which causes it to be a monomeric form at $\text{pH} < 3.7$ (Fig. 6a) and a zwitterionic form (Fig. 6b) at $\text{pH} > 3.7$.

According to the pH_{pzc} concept, at low pH, the surface of the adsorbent is highly positively charged, which should lead to the repulsion of the cationic dye molecules and cause a decrease in adsorption efficiency. On the other hand, when the solution pH increases above pH_{pzc} , the surface of the adsorbent gets negatively charged, and electrostatic attraction forces between the cationic RhB and the adsorbent surface should promote adsorption. This pH

Table 6 Comparison of Rhodamine B adsorption on various low-cost materials

Sorbent	q_m (mg/g)	References
Devonian sand	0.349	This study
Chalcedonite	2.701	This study
Halloysite	4.252	This study
Zeolite	6.964	This study
Sugar cane bagasse	1.250	Abou-Gamra and Medien (2013)
Raw walnut shells	2.292	Shah et al. (2013)
Fly ash	2.300	Khan et al. (2009)
Ultrasound treated halloysite	4.010	Wierzbicka et al. (2022)
Acid-activated halloysite	6.290	Wierzbicka et al. (2022)
Pomegranate peels ground powder	7.370	Saigl and Ahmed (2021)
Kaolin	7.760	He et al. (2022)
Modified zeolite (mordenite)	7.955	Cheng et al. (2016)
Diatomite	8.130	Koyuncu and Kul (2014)
Organo-modified halloysite	8.530	Wierzbicka et al. (2022)
Orange peel powder	10.17	Daouda et al. (2019)
Kaolin-sodium bentonite	11.26	He et al. (2022)
Kaolin-organic bentonite	12.68	He et al. (2022)
Sugarcane fiber	15.98	Parab et al. (2009)
Pristine bentonite	17.01	de Morais Pinos et al. (2022)
Modified bentonite (CTA-DAPTMS)	18.78	de Morais Pinos et al. (2022)
Rice husk	28.13	Jain et al. (2007)
Moroccan natural clay bentonite	29.33	Lamrani et al. (2023)
<i>Araucaria angustifolia</i> sterile bracts	36.70	Matias et al. (2020)
Cardboard	50.25	Kant et al. (2014)
Charred endocarp of dika nut	52.90	Inyinbor et al. (2017)
Coir pith	55.54	Parab et al. (2009)
Perlite	67.93	Vijayakumar et al. (2012)
Beech sawdust	70.40	Witek-Krowiak et al. (2010)
Brazilian natural bentonite	77.30	Zimmermann et al. (2016)
<i>Casuarina equisetifolia</i> needle	82.34	Kooh et al. (2016)
<i>Thespesia populnea</i> bark	103.1	Prabakaran and Arivoli (2012)
Java bentonite	116.3	Hakim et al. (2023)
Modified Na-bentonite	136.9	Hakim et al. (2023)
Baryte	163.9	Vijayakumar et al. (2010)
Modified NH-bentonite	192.3	Hakim et al. (2023)
Tannery residual biomass	212.7	Anandkumar and Mandal (2011)
Modified bentonite (CTA)	284.4	de Morais Pinos et al. (2022)

Fig. 6 Cationic (a) and zwitterionic (b) forms of Rhodamine B

dependency of adsorption was reported for RhB removal on charred endocarp of dika nut (Inyinbor et al., 2017), perlite (Vijayakumar et al., 2012), and barite (Vijayakumar et al., 2010). However, as evidenced in this study, dye adsorption is completely different depending on the pH, which suggests that the adsorption process of RhB is a complex issue. Generally, dyes are adsorbed mainly through hydrophobic and electrostatic attractions and hydrogen bonding between the dye molecules and the adsorbent surface. Yu et al. (2013) proposed possible interactions between the adsorbent (zeolite modified with graphene oxide) and Rhodamine B molecules. In an acidic environment, at pH below pK_a and pH_{pzc} , RhB can interact with the adsorbent surface through electrostatic, hydrophobic, and hydrogen bond interactions. At higher pH (above pK_a and pH_{pzc}), attractive and repulsive electrostatic interactions, as well as hydrogen bond interactions, are possible.

In this study, the maximum RhB adsorption on all tested materials was recorded at pH 2.2 (Fig. 5), at which the dye molecules exist in cationic and monomeric forms, and the adsorbent surface is positively charged. This is contradictory to the pH_{pzc} theory, thus suggesting that electronic interaction is not the major adsorbate–adsorbent interaction force and that other attraction forces, such as hydrophobic–hydrophobic interaction, could be more dominant. High adsorption at pH 2.2 can probably be attributed to the fact that low pH increased protonation of the adsorbent; this contributed to RhB diffusion and generated a larger number of active sites on the adsorbent surfaces, thereby enhancing surface adsorption (Jain et al., 2007). As the pH of the RhB solution increased, adsorption decreased. At higher pH, the RhB molecules exist in zwitterionic forms (Fig. 6b), and the surface of the adsorbent is negatively charged. The lower uptake may, in part, be due to the repulsive electrostatic interactions between negative charges on the surface of the adsorbents and hydroxyl ions in the dye molecules. Moreover, at higher pH, the attractive electrostatic interaction between the carboxyl and xanthene groups of RhB monomers may increase the aggregation of Rhodamine B to form bigger molecular forms (dimers). The adsorption of these large dye molecules (dimers) becomes unable to enter into the pore structure of the adsorbent surface resulting in an adsorption capacity decrease. Aggregation of dye molecules at high pH also explains in some way the

favorable adsorption of RhB in an acidic environment — smaller monomeric RhB occurring at $pH < pK_a$ may diffuse into micropores of the adsorbent more readily than the dimer form occurring at $pH > pK_a$. The same behavior — decrease in adsorption with increasing pH — was also reported in the studies of RhB removal by sugar cane bagasse (Abou-Gamra & Medien, 2013), raw walnut shells (Shah et al., 2013), rice husk (Jain et al., 2007), *Araucaria angustifolia* sterile bracts (Matias et al., 2020), *Casuarina equisetifolia* needles (Kooch et al., 2016), and carboxy-GO/zeolite (Yu et al., 2013).

4 Conclusions

Four mineral materials, i.e., zeolite, halloysite, chalcidonite, and Devonian sand, were compared based on their adsorption capacity of Rhodamine B from aqueous solutions. Adsorption equilibrium and kinetics were studied. The Freundlich, Langmuir, and Sips isotherm models were applied to the equilibrium data of the dye adsorption. The results show that the equilibrium data fitted well with the Freundlich equilibrium. Monolayer adsorption capacities of Ze, Ha, Ch, and DS were at 6.964, 4.252, 2.701, and 0.349 mg/g, respectively. Two kinetic models, pseudo-first-order and pseudo-second-order, were used to test the adsorption kinetics of RhB on the applied materials. The data were best fitted to the pseudo-second-order kinetic model. The adsorption capabilities of the tested materials were strongly dependent on the pH of the solution. Acidic pH = 2.2 was found to be the best pH for the elimination of the dye, and the adsorption efficiency decreased with the pH increase. This phenomenon suggests that hydrophobic–hydrophobic interactions occur between the surfaces of the mineral materials and RhB molecules. The results of these investigations indicate that selected natural materials can be employed as alternatives to commercial adsorbents in Rhodamine B removal from aqueous solutions.

Data Availability All data generated or analyzed during this study are included in this article.

Declarations

Conflict of Interest The authors declare no competing interests.

Open Access This article is licensed under a Creative Commons Attribution 4.0 International License, which permits use, sharing, adaptation, distribution and reproduction in any medium or format, as long as you give appropriate credit to the original author(s) and the source, provide a link to the Creative Commons licence, and indicate if changes were made. The images or other third party material in this article are included in the article's Creative Commons licence, unless indicated otherwise in a credit line to the material. If material is not included in the article's Creative Commons licence and your intended use is not permitted by statutory regulation or exceeds the permitted use, you will need to obtain permission directly from the copyright holder. To view a copy of this licence, visit <http://creativecommons.org/licenses/by/4.0/>.

References

- Abou-Gamra, Z. M., & Medien, H. A. A. (2013). Kinetic, thermodynamic and equilibrium studies of Rhodamine B adsorption by low cost biosorbent sugar cane bagasse. *European Chemical Bulletin*, 2(7), 417–422.
- Adebiyi, F. M., & Ayeni, D. A. (2021). Chemical speciation, bioavailability and risk assessment of potentially toxic metals in soils around petroleum product marketing company as environmental degradation indicators. *Petroleum Research (in Press)*. <https://doi.org/10.1016/j.ptlrs.2021.08.006>
- Al-Ghouti, M. A., & Da'ana, D. A. (2020). Guidelines for the use and interpretation of adsorption isotherm models: A review. *Journal of Hazardous Materials*, 393, 122383. <https://doi.org/10.1016/j.jhazmat.2020.122383>
- Anandkumar, J., & Mandal, B. (2011). Adsorption of chromium(VI) and Rhodamine B by surface modified tannery waste: Kinetic, mechanistic and thermodynamic studies. *Journal of Hazardous Materials*, 186, 1088–1096. <https://doi.org/10.1016/j.jhazmat.2010.11.104>
- Ayawei, N., Ebelegi, A. N., & Wankasi, D. (2017). Modelling and interpretation of adsorption isotherms. *Journal of Chemistry*, 2017, 1–11. <https://doi.org/10.1155/2017/3039817>
- Bandura, L., Białoszewska, M., Malinowski, S., & Franus, W. (2021). Adsorptive performance of fly ash-derived zeolite modified by β -cyclodextrin for ibuprofen, bisphenol A and caffeine removal from aqueous solutions—equilibrium and kinetic study. *Applied Surface Science*, 562, 150160. <https://doi.org/10.1016/j.apsusc.2021.150160>
- Bandura, L., Kołodyńska, D., & Franus, W. (2017). Adsorption of BTX from aqueous solutions by Na-P1 zeolite obtained from fly ash. *Process Safety and Environment Protection*, 109, 214–223. <https://doi.org/10.1016/j.psep.2017.03.036>
- Bernasconi, C., Demetrio, P. M., Alonso, L. L., Mac Loughlin, T. M., Cerdá, E., Sarandón, S. J., & Marino, D. J. (2021). Evidence for soil pesticide contamination of an agroecological farm from a neighboring chemical-based production system. *Agriculture, Ecosystems & Environment*, 313, 107341. <https://doi.org/10.1016/j.agee.2021.107341>
- Birch, G. F., Fayeli, F. S., & Matthai, C. (2005). Efficiency of an infiltration basin in removing contaminants from urban storm water. *Environmental Monitoring and Assessment*, 101, 145–155.
- Bizi, M., & El Bachra, F. E. (2020). Evaluation of the ciprofloxacin adsorption capacity of common industrial minerals and application to tap water treatment. *Powder Technology*, 362, 323–333. <https://doi.org/10.1016/j.powtec.2019.11.047>
- Cheng, W.-Y., Li, N., Pan, Y.-Z., & Jin, L.-H. (2016). The adsorption of Rhodamine B in water by modified zeolites. *Modern Applied Science*, 10(5), 67–76. <https://doi.org/10.5539/mas.v10n5p67>
- Daouda, A., Honorine, A. T., Bertrand, N. G., & Richard, D. (2019). Adsorption of Rhodamine B onto orange peel powder. *American Journal of Chemistry*, 9(5), 142–149. <https://doi.org/10.5923/j.chemistry.20190905.02>
- de Morais Pinos, J. Y., de Melo, L. B., de Souza, S. D., Marçal, L., & de Faria, E. H. (2022). Bentonite functionalized with amine groups by the sol-gel route as efficient adsorbent of rhodamine-B and nickel (II). *Applied Clay Science*, 223, 106494. <https://doi.org/10.1016/j.clay.2022.106494>
- El Sayed, E. E. (2018). Natural diatomite as an effective adsorbent for heavy metals in water and wastewater treatment (a batch study). *Water Science*, 32(1), 32–43. <https://doi.org/10.1016/j.wsj.2018.02.001>
- Fronczyk, J. (2017). Artificial road runoff water treatment by a pilot-scale horizontal permeable treatment zone. *Ecological Engineering*, 107, 198–207. <https://doi.org/10.1016/j.ecoleng.2017.07.025>
- Fronczyk, J. (2020). Properties of reactive materials for application in runoff water treatment systems. *Journal of Ecological Engineering*, 21(8), 185–197. <https://doi.org/10.12911/22998993/126988>
- Fronczyk, J., & Mumford, K. A. (2019). The impact of temperature on the removal of inorganic contaminants typical of urban stormwater. *Applied Sciences*, 9, 1273. <https://doi.org/10.3390/app9071273>
- Fronczyk, J., & Radziemska, M. (2016). Removal of copper(II) ions from groundwater using powdered Devonian dolomite in permeable reactive barriers. *Carpathian J Earth Environ Sci*, 11(1), 113–121.
- Fronczyk, J., Radziemska, M., & Jeznach, J. (2014). Evaluation of diatomite and chalcedonite as reactive materials protecting groundwater in traffic infrastructure. *Fresenius Environmental Bulletin*, 23(12b), 3331–3339.
- Fronczyk, J., & Garbulewski, K. (2013). Evaluation of zeolite-sand mixtures as reactive materials protecting groundwater at waste disposal sites. *Journal of Environmental Sciences*, 25(9), 1764–1772. [https://doi.org/10.1016/S1001-0742\(12\)60270-8](https://doi.org/10.1016/S1001-0742(12)60270-8)
- Fuerhacker, M., Haile, T. M., Monai, B., & Mentler, A. (2011). Performance of a filtration system equipped with filter media for parking lot runoff treatment. *Desalination*, 275, 118–125. <https://doi.org/10.1016/j.desal.2011.02.041>
- Hakim, Y. M., Mohadi, R., & Mardiyanto, Royani I. (2023). Ammonium-assisted intercalation of Java bentonite as effective of cationic dye removal. *Journal of Ecological Engineering*, 24(2), 184–195. <https://doi.org/10.12911/22998993/156665>
- He, H., Chai, K., Wu, T., Qiu, Z., Wang, S., & Hong, J. (2022). Adsorption of Rhodamine B from simulated waste water onto kaolin-bentonite composites. *Materials*, 15, 4058. <https://doi.org/10.3390/ma15124058>

- Inyinbor, A. A., Adekola, F. A., & Olatunji, G. A. (2017). Liquid phase adsorptions of Rhodamine B dye onto raw and chitosan supported mesoporous adsorbents: Isotherms and kinetics studies. *Applied Water Science*, 7, 2297–2307. <https://doi.org/10.1007/s13201-016-0405-4>
- Jain, R., Mathur, M., Sikarwar, S., & Mittal, A. (2007). Removal of the hazardous dye rhodamine B through photocatalytic and adsorption treatments. *Journal of Environmental Management*, 85, 956–964. <https://doi.org/10.1016/j.jenvman.2006.11.002>
- Kant, A., Gajjon, P., & Nadeem, U. (2014). Adsorption studies of Rhodamine B from aqueous solution using low cost material: Equilibrium and kinetics studies. *International Journal of Current Research*, 6(8), 7790–7796.
- Khan, T. A., Ali, I., Singh, V. V., & Sharma, S. (2009). Utilization of fly ash as low-cost adsorbent for the removal of methylene blue, malachite green and Rhodamine B dyes from textile wastewater. *Journal of Environmental Protection Science*, 3(1), 11–22.
- Kooh, M. R. R., Dahri, M. K., & Lim, L. B. L. (2016). The removal of rhodamine B dye from aqueous solution using *Casuarina equisetifolia* needles as adsorbent. *Cogent Environmental Science*, 2, 1140553. <https://doi.org/10.1080/23311843.2016.1140553>
- Koyuncu, M., & Kul, A. R. (2014). Thermodynamics and adsorption studies of dye (rhodamine-B) onto natural diatomite. *Physicochemical Problems of Mineral Processing*, 50(2), 631–643. <https://doi.org/10.5277/ppmp140217>
- Kuśmierk, K., Dąbek, L., & Świątkowski, A. (2020). Comparative study on the adsorption kinetics and equilibrium of common water contaminants onto bentonite. *Desalination Water Treat*, 186, 373–381. <https://doi.org/10.5004/dwt.2020.25476>
- Lamrani, O., Tanji, K., Redouane, H., Fahoul, Y., Belkasm, M., & Boushaba, A. (2023). Efficient adsorption of RhB using Moroccan natural clay: Equilibrium, kinetic, thermodynamic, and theoretical study. *Euro-Mediterranean Journal for Environmental Integration*, 8, 303–318. <https://doi.org/10.1007/s41207-023-00380-4>
- Liu, K., Li, H., Wang, Y., Gou, X., & Duan, Y. (2015). Adsorption and removal of rhodamine B from aqueous solution by tannic acid functionalized graphene. *Colloids and Surfaces A: Physicochem Eng Aspects*, 477, 35–41. <https://doi.org/10.1016/j.colsurfa.2015.03.048>
- Long, Z., Zhu, H., Bing, H., Tian, X., Wang, Z., Wan, X., & Wu, Y. (2021). Contamination, sources and health risk of heavy metals in soil and dust from different functional areas in an industrial city of Panzhihua City, Southwest China. *Journal of Hazardous Materials*, 420, 126638. <https://doi.org/10.1016/j.jhazmat.2021.126638>
- Matias, C. A., Oliveira, L. J. G. G. D., Geremias, R., & Stolberg, J. (2020). Biosorption of Rhodamine B from aqueous solution using *Araucaria angustifolia* sterile bracts. *Revista Internacional de Contaminación Ambiental*, 36(1), 97–104. <https://doi.org/10.20937/RICA.2020.36.53282>
- Oszczak-Nowińska, A., Świątkowski, A., Fronczyk, J., & Fuks, L. (2021). Adsorption of Cs-137 and Am-241 ions from aqueous solutions on bentonites. *Desalination Water Treat*, 214, 433–439. <https://doi.org/10.5004/dwt.2021.26746>
- Parab, H., Sudersanan, M., Shenoy, N., Pathare, T., & Vaze, B. (2009). Use of agro-industrial wastes for removal of basic dyes from aqueous solutions. *Clean*, 37(12), 963–969. <https://doi.org/10.1002/clen.200900158>
- Piol, M. N., Paricoto, M., Saralegui, A. B., Basack, S., Vullo, D., & Boeykens, S. P. (2019). Dolomite used in phosphate water treatment: Desorption processes, recovery, reuse and final disposition. *Journal of Environmental Management*, 237, 359–364. <https://doi.org/10.1016/j.jenvman.2019.02.085>
- Prabakaran, R., & Arivoli, S. (2012). Equilibrium isotherm, kinetic and thermodynamic studies of Rhodamine B adsorption using *Thespesia populnea* bark. *Journal of Chemical and Pharmaceutical Research*, 4(10), 4550–4557.
- Radziemska, M., Beś, A., Gusiati, Z. M., Cerdà, A., Jeznach, J., Mazur, Z., & Brtnický, M. (2020a). Assisted phytostabilization of soil from a former military area with mineral amendments. *Ecotoxicology and Environmental Safety*, 188, 109934. <https://doi.org/10.1016/j.ecoenv.2019.109934>
- Radziemska, M., Beś, A., Gusiati, Z. M., Majewski, G., Mazur, Z., Bilgin, A., Jaskulska, I., & Brtnický, M. (2020b). Immobilization of potentially toxic elements (PTE) by mineral-based amendments: Remediation of contaminated soils in post-industrial sites. *Minerals*, 10(2), 87. <https://doi.org/10.3390/min10020087>
- Radziemska, M., Koda, E., Vaverková, M. D., Gusiati, Z. M., Cerdà, A., Brtnický, M., & Mazur, Z. (2019). Soils from an iron and steel scrap storage yard remediated with aided phytostabilization. *Land Degradation and Development*, 30(2), 202–211. <https://doi.org/10.1002/ldr.3215>
- Reczek, L., Michel, M. M., Siwiec, T., & Żukowska, E. (2014). Sorpcja jonów ołowiu (II) na wybranych materiałach filtracyjnych stosowanych w technologii uzdatniania wody. *Przemysł Chemiczny*, 93(11), 1978–1982. in Polish.
- Saigl, Z. M., & Ahmed, A. M. (2021). Separation of Rhodamine B dye from aqueous media using natural pomegranate peels. *Indonesian Journal of Chemistry*, 21(1), 212–224. <https://doi.org/10.22146/ijc.58592>
- Shah, J., Rasul Jan, M., Haq, A., & Khan, Y. (2013). Removal of Rhodamine B from aqueous solutions and wastewater by walnut shells: Kinetics, equilibrium and thermodynamics studies. *Frontiers of Chemical Science and Engineering*, 7(4), 428–436. <https://doi.org/10.1007/s11705-013-1358-x>
- Sieczka, A. (2015). Badania laboratoryjne dyspersyjności i pęcznienia wybranych bentonitów stosowanych jako bariery izolacyjne obiektów budowlanych. *Acta Scientiarum Polonorum. Architectura*, 14(4), 61–73. in Polish.
- Skjolding, L. M., LvG, J., Dyhr, K. S., Köppl, C. J., McKnight, U. S., Bauer-Gottwein, P., Mayer, P., Bjerg, P. L., & Baun, A. (2021). Assessing the aquatic toxicity and environmental safety of tracer compounds Rhodamine B and Rhodamine WT. *Water Research*, 197, 117109. <https://doi.org/10.1016/j.watres.2021.117109>
- Suthersan, S. S., Horst, J., Schnobrich, M., Welty, N., & McDonough, J. (2016). *Remediation engineering: Design concepts*. CRC Press.
- Tan, K. L., & Hameed, B. H. (2017). Insight into the adsorption kinetics models for the removal of contaminants

- from aqueous solutions. *Journal of the Taiwan Institute of Chemical Engineers*, 74, 25–48. <https://doi.org/10.1016/j.jtice.2017.01.024>
- Trach, Y., Tytkowska-Owerko, M., Reczek, L., & Michel, M. M. (2021). Comparison the adsorption capacity of Ukrainian tuff and basalt with zeolite–manganese removal from water solution. *Journal of Ecological Engineering*, 22(3), 161–168. <https://doi.org/10.12911/22998993/132605>
- Ukaogo, P.O., Ewuzie, U., Onwuka, C. V. (2020). Environmental pollution: Causes, effects, and the remedies. In: *Microorganisms for sustainable environment and health*, 21, Elsevier, 419–429. <https://doi.org/10.1016/C2018-0-05025-2>.
- Vieira, Y., Leichtweis, J., Foletto, E. L., & Silvestri, S. (2020). Reactive oxygen species-induced heterogeneous photocatalytic degradation of organic pollutant Rhodamine B by copper and zinc aluminate spinels. *Journal of Chemical Technology and Biotechnology*, 95, 791–797. <https://doi.org/10.1002/jctb.6267>
- Vignola, R., Bagatin, R., Alessandra De Folly, D., Massara, E. P., Ghisletti, D., Millini, R., & Sisto, R. (2011). Zeolites in a permeable reactive barrier (PRB): One-year of field experience in a refinery groundwater. Part 2: Zeolite characterization. *Journal of Chemical Engineering*, 178, 210–216. <https://doi.org/10.1016/j.cej.2011.10.050>
- Vijayakumar, G., Tamilarasan, R., & Dharmendirakumar, M. (2012). Adsorption, kinetic, equilibrium and thermodynamic studies on the removal of basic dye Rhodamine-B from aqueous solution by the use of natural adsorbent perlite. *Journal of Materials and Environmental Science*, 3(1), 157–170.
- Vijayakumar, G., Yoo, C. K., Elango, K. G. P., & Dharmendirakumar, M. (2010). Adsorption characteristics of Rhodamine B from aqueous solution onto baryte. *Clean*, 38(2), 202–209. <https://doi.org/10.1002/clen.200900125>
- Wang, Y., Wei, H., Wang, Y., Peng, C., & Dai, J. (2021). Chinese industrial water pollution and the prevention trends: An assessment based on environmental complaint reporting system (E CRS). *Alexandria Engineering Journal*, 60(6), 5803–5812. <https://doi.org/10.1016/j.aej.2021.04.015>
- Wierzbicka, E., Kuśmierk, K., Świątkowski, A., & Legocka, I. (2022). Efficient rhodamine B dye removal from water by acid- and organo-modified halloysites. *Minerals*, 12, 350. <https://doi.org/10.3390/min12030350>
- Witek-Krowiak, A., Mitek, M., Pokomeda, K., Szafran, R. G., & Modelski, S. (2010). Biosorption of cationic dyes by beech sawdust I. Kinetics and equilibrium modelling. *Chemical Engineering and Processing*, 31, 409–420.
- Yu, Y., Murthy, B. N., Shapter, J. G., Constantopoulos, K. T., Voelcker, N. H., & Ellis, A. V. (2013). Benzene carboxylic acid derivatized graphene oxide nanosheets on natural zeolites as effective adsorbents for cationic dye removal. *Journal of Hazardous Materials*, 260, 330–338. <https://doi.org/10.1016/j.jhazmat.2013.05.041>
- Zimmermann, B. M., Dotto, G. L., Kuhn, R. C., Mazutti, M. A., Treichel, H., & Foletto, E. L. (2016). Adsorption of hazardous dye Rhodamine B onto Brazilian natural bentonite. *International Journal of Environmental Technology and Management*, 19(1), 1–15.

Publisher's Note Springer Nature remains neutral with regard to jurisdictional claims in published maps and institutional affiliations.